

Jet tomography in heavy-ion collisions - Challenges, Results, and Open Problems

Barbara Betz

Abstract Over the past 30 years, jet observables have proven to provide important information about the quark-gluon plasma created in heavy-ion collisions. I review the challenges, results, and open problems of jet physics in heavy-ion collisions, discussing the main ideas as well as some most recent results focussing on two major jet observables, the nuclear modification factor and the high- p_T elliptic flow.

1 Jets in heavy-ion collisions

Relativistic high-energy heavy-ion collisions offer the unique possibility to study matter experimentally under extreme conditions of high temperature and densities in the laboratory. One of the main challenges is to probe the quark-gluon plasma (QGP) created in such heavy-ion collisions. One set of observables is based on *jets*, sprays of particles that are produced back-to-back due to the conservation of energy and momentum. Those jets propagate through the dense matter formed while depositing energy. As this jet-energy loss inevitably leads to an attenuation of the jet [1, 2, 3, 4, 5] this concept is referred to as **jet quenching**.

The breakthrough of studying jets in heavy-ion collisions came with the start of the Relativistic Heavy Ion Collider (RHIC) in 2000 [6, 7, 8, 9]. By studying the azimuthal distribution of the back-to-back jets in Au+Au collisions at RHIC, it could be shown that this part of the jet which propagates through the hot and dense matter is suppressed (or **quenched**) as compared to measurements in proton+proton (p+p) or deuteron+gold (d+Au) collisions [10, 11]. This result is considered as a clear signal that at RHIC energies the hot and dense QGP medium is only created in heavy-ion collisions.

Barbara Betz
Institut für Theoretische Physik, Goethe Universität, Frankfurt am Main, Germany, e-mail: betz@th.physik.uni-frankfurt.de

Over many years, the actual evolution of the jet, the creation of shock waves and possible Mach cones [12, 13, 14], have been discussed extensively in literature. However, in the following I will focus on **jet tomography**, an approach pursuing the concept of jet quenching:

By studying jet quenching, one should be able to characterize some properties of the medium created. This idea is used e.g. in medicine by x-ray tomography where a beam of particles traverses a medium (e.g. the human body). This beam is deflected and/or absorbed and its remnants are measured in a detector. Finally, this measurement leads to an image of the interior of the human's body. Likewise, one aims to getting an image of the interior of a heavy-ion collision by performing jet tomography.

The basic idea of jet quenching and jet tomography has been applied in heavy-ion collisions since the 1990's. On the theory side, it has lead to various jet-quenching models: GLV, DGLV, WHDA, AMY, ASW, ... [15, 16, 17, 18, 19, 20, 21].

1.1 Major jet observables

Jet quenching is predominantly quantified by the nuclear modification factor (R_{AA}) which is the ratio of the number of particles created in a nucleus+nucleus (A+A) collision scaled to the number of particles created in a p+p collision and the number of collisions N_{coll} :

$$R_{AA}(p_T) = \frac{dN_{AA}/dp_T}{N_{\text{coll}}dN_{pp}/dp_T} \quad (1)$$

Usually, this ratio is given as a function of the transverse momentum p_T . If a heavy-ion collision was a pure superposition of a p+p collisions then $R_{AA} = 1$. However, if there is jet quenching then $R_{AA} < 1$.

One of the major results obtained at RHIC [22, 23] was to show that the measured nuclear modification factor for pions, the predominant species of particles measured in Au+Au collisions, is $R_{AA} \sim 0.2$ which is significantly below 1.

With this measurement, the predicted jet suppression [1, 2, 3, 24] was first observed at RHIC and it is considered as a signal for the creation of an opaque matter, the quark-gluon plasma [25, 26].

A second major jet observable, the high- p_T elliptic flow (v_2), is based on a characteristic observable of the background medium, the elliptic flow v_2 . Most A+A collisions show an offset. If the particles in the overlap region, where the hot and dense QGP medium is formed, interact then gradients will lead to a preferred emission.

By comparison to hydrodynamic simulations [27], it was shown that the background medium shows a preferred direction resulting an asymmetry which is quantified by the 2nd Fourier coefficient of the angular distribution, the elliptic flow v_2 :

$$\frac{dN}{d\phi} = \frac{N}{2\pi} \left[1 + 2 \sum_{n=1}^{\infty} v_n \cos(n\phi) \right]. \quad (2)$$

Jets created in the overlap region that interact with the medium will certainly be affected by the preferred emission of the background medium, resulting in a preferred emission of the high- p_T particles (jets). Thus, even though the underlying physics leading to this preferred emission is different, this observed preferred emission is referred to as *high- p_T elliptic flow*.

2 Jet tomography – a challenge in heavy-ion collisions

Usually the jet-energy loss in heavy-ion collisions is considered to be very similar to tomography of X-rays routinely used in medicine. However, both procedures are indeed quite different.

In contrast to an ideal tomography (for simplicity one might think of an x-ray tomography mentioned above), a heavy-ion collision misses [28]

1. a controlled flow of penetrating particles,
2. an established dynamical theory of the energy loss,
3. and a non-moving, non-fluctuating background medium.

Of course, this does *not* imply that jet tomography cannot be done in heavy-ion collisions but it indicates that conclusions might not be as straightforward as they seem.

3 Immediate consequences from the first results at the LHC

Before the Large Hadron Collider (LHC) was turned on in 2010, one of main questions discussed was if the correct description of a jet-energy loss in heavy-ion collisions is done by using perturbative QCD (pQCD) or by applying the Anti-de-Sitter/Conformal Field Theory (AdS/CFT) correspondence [15, 16, 17, 18, 19, 20, 21, 29, 30, 31, 32, 33].

Pre-LHC runs performed at RHIC [34] indicated that the measured nuclear modification factor and the high- p_T elliptic flow can only be described **simultaneously** if a squared path-length dependence, $dE/dx = dE/d\tau \sim \tau^2$, is considered. This squared path-length dependence points to an AdS/CFT-like energy loss while a pQCD-like jet-energy loss is assumed to have a linear path-length dependence, $dE/dx = dE/d\tau \sim \tau$.

Right after the start of the LHC, a remarkable result was obtained for the nuclear modification factor. In contrast to early pQCD-based predictions [24], the R_{AA} showed an unexpected similarity for measurements at RHIC and LHC in the region $10 < p_T < 20$ GeV.

These measurements indicate that there is a *surprising QGP-transparency* [35, 36, 37] for LHC energies. It suggests that the jet-medium coupling at LHC energies is smaller than at RHIC energies which points to a running-coupling effect consistent with pQCD but not with AdS/CFT.

Besides this, *conformal* AdS/CFT energy loss was expected to yield a flat R_{AA} [38]. However, the distinct slope of the pQCD prediction for the nuclear modification factor at LHC energies given in Ref. [24] was shown to be correct, resulting in the question if (conformal) AdS/CFT was ruled out by the first data of the LHC and how to resolve the puzzle connected to the pre-LHC runs.

4 The BBMG model

To investigate the measured jet-energy loss at RHIC and LHC energies, we developed a generic jet-energy loss model (for convenience referred to as BBMG model) over the past few years [36, 39, 40]. This model is based on the following ansatz of the jet-energy loss:

$$\frac{dE}{d\tau} = -\kappa E^a \tau^z T^{c=(2+z-a)} \zeta_q \Gamma_f, \quad (3)$$

with the jet-medium coupling κ , jet energy E , the path-length τ , and the temperature density of the background medium T .

Jet-energy loss fluctuations are included via the distribution

$$f_q(\zeta_q) = \frac{(1+q)}{(q+2)^{1+q}} (q+2 - \zeta_q)^q \quad (4)$$

which allows for an easy interpolation between non-fluctuating ($\zeta_{q=-1} = 1$) distributions and those ones increasingly skewed towards small $\zeta_{q>-1} < 1$ [40].

The background flow fields are incorporated via the flow factor

$$\Gamma_f = \gamma_f [1 - v_f \cos(\phi_{\text{jet}} - \phi_{\text{flow}})] \quad (5)$$

[41, 42, 43, 44] with the background flow velocities v_f and the γ -factor

$$\gamma_f = 1/\sqrt{1 - v_f^2}. \quad (6)$$

ϕ_{jet} is the jet angle w.r.t. the reaction plane and $\phi_{\text{flow}} = \phi_{\text{flow}}(\mathbf{x}, t)$ is the corresponding local azimuthal angle of the background flow fields.

Even though this model is quite simple and not based on first-principles calculations, it has offered the possibility to explore the jet physics in high-energy heavy-ion collisions to a surprising quantitative accuracy. Besides that, the results obtained via the BBMG model have always been cross-checked with the CUJET model [45, 46, 47] which based on pQCD calculations up to 10 orders in opacity.

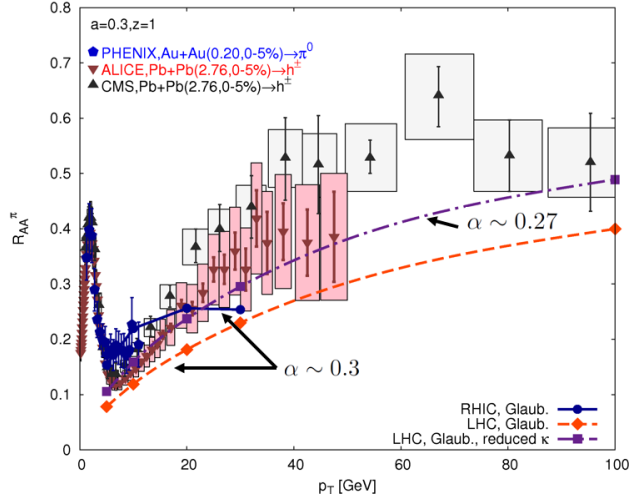


Fig. 1 The early results for the nuclear modification factor measured at RHIC and LHC [51, 52, 53] compared to calculations of an early version of the BBMG model given by $dE/d\tau = -\kappa E^{a=0.3} \tau^{z=1} T^{c=2.7}$ without jet-energy loss fluctuations and background flow. The results for a coupling constant of $\alpha = 0.3$ reproduce the measured data at RHIC energies (blue solid line) but overquench at LHC energies (orange dashed line). For a moderately reduced coupling of $\alpha = 0.27$, the nuclear modification factor for pions at LHC energies (magenta dashed-dotted line) is preferred.

The BBMG model interpolates between pQCD-based and AdS/CFT-inspired jet-energy loss algorithms with a linear and a squared path-length z , respectively, and has been coupled to state-of-the-art hydrodynamic and parton cascade background media [48, 49, 50].

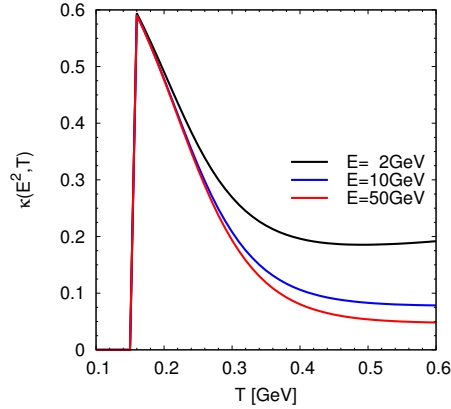
By calculating the nuclear modification factor and the high- p_T elliptic flow for RHIC and LHC, the jet-medium coupling, the jet-energy dependence, the path-length dependence, and the impact of the background have been explored [36, 39, 40].

In particular, we have been able to show that a moderate reduction of the jet-medium coupling is needed to describe the LHC nuclear modification factor at LHC energies, see Fig. 1. We could also prove that the rapid rise of the nuclear modification factor at LHC energies rules out any model with $dE/dx \sim E^{a>1/3}$. This rapid rise can easily be seen from Fig. 1. Please note that $a = 1/3$ is the lower bound of the falling-string scenario, while $a = 0$ is referred to a pQCD-scenario [39].

By performing a detailed survey [40], we demonstrated that a pQCD-based scenario with the parameters $a = 0, z = 1, c = 3$ in Eq. (3) describes the measured nuclear modification factor and the high- p_T elliptic flow within the uncertainties of the bulk evolution if a running jet-medium coupling is considered. Those uncertainties are given e.g. by the initial state and the viscosity of the background medium.

In case of a *conformal* AdS-scenario with a squared path-length dependence, however, the nuclear modification factor is clearly overquenched [40]. The reason is that a conformal AdS-scenario is characterized by a fixed jet-medium coupling

Fig. 2 The jet-medium coupling $\kappa(E^2, T)$, generalized in Ref. [45], as a function of the jet energy E and the medium temperature T . There is no interaction below $T_c = 0.16$ GeV as it is assumed that the medium is converted into hadrons below this temperature.



since a conformal theory does not have any additional scale which can run. Thus, we concluded [40] that a *conformal* scenario is ruled out by the rapid rise of the measured $R_{AA}(p_T)$.

In contrast, a *non-conformal* AdS-scenario [54, 55] allowing for a running of the jet-medium coupling, does lead to similar results as the pQCD calculations [40]. Thus, we observed that a linear and a squared path-length dependence lead to similar results for the nuclear modification factor and the high- p_T elliptic flow and does not allow for an any disentangling of a possible pQCD and AdS-scenario [40]. One of the main open challenges is to find a possible new observable which breaks this degeneracy.

5 The high- p_T v_2 problem

As mentioned above, we showed in Ref. [40] that a pQCD scenario describes the measured data within the theoretical and experimental uncertainties given. However, our results are at the lower end of the measured error bars. This is in line with other jet-energy loss models. While various different models can describe the R_{AA} , the high- p_T is rather challenging and up to a factor of 2 too small as compared to the data [34, 56, 57].

Ref. [45] suggested that a jet-medium coupling including non-perturbative effects around the phase transition at $T_c \sim 160$ GeV and depending both on the energy of the jet and the temperature of the background medium, $\kappa(E^2, T)$, resolves the high- p_T v_2 problem and leads to a simultaneous prescription of both the R_{AA} and the high- p_T v_2 .

Since the jet-medium coupling $\kappa(E^2, T)$ has been generalized to an analytic form [45] (which is plotted in Fig. 2), it can easily be included in the BBMG model given by Eq. (3). In Ref. [58] we showed that the energy and temperature-dependent jet-medium coupling improves the description of the high- p_T elliptic flow drastically,

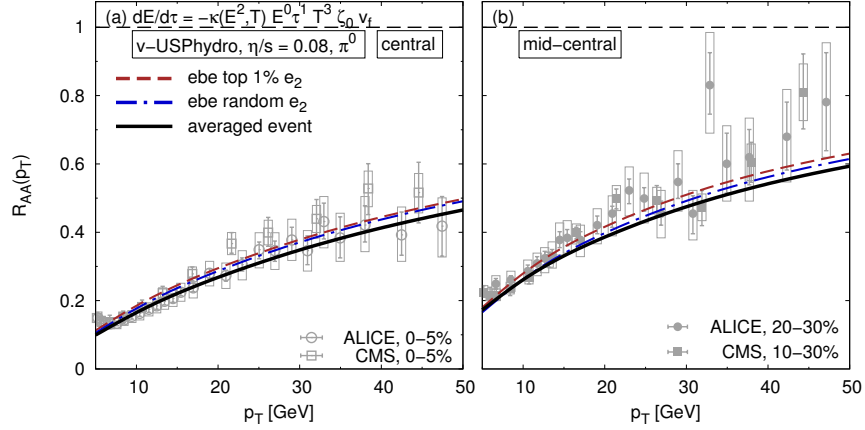


Fig. 3 The nuclear modification factor for central and mid-central events measured at $\sqrt{2.75}$ TeV LHC energy [60, 61] compared to the three Glauber e_2 -eccentricity selections of the centrality classes 0-5% (left) and 20-30% (right).

independently of a hydrodynamic or parton cascade background medium considered.

6 SHEE – Soft-Hard Event Engineering

To further study the impact of the background on the high- p_T elliptic flow, in particular the impact of the e_2 -eccentricity selection (determining the centrality of a collision) within a given centrality class, we have recently started to compare various selected soft (low- p_T background) and hard (high- p_T jet) events [59].

The wide low- p_T distributions measured by the ATLAS collaboration [62] have proven that background models must render both the $\langle \text{low-}p_T v_n \rangle$ and the correct fluctuations within a centrality class.

For SHEE [63], we coupled the (hydrodynamic) v-USPhydro code [64, 65] to the BBMG model. 15,000 Glauber initial conditions are generated and three different events are selected:

1. 150 events with random e_2 -eccentricity,
2. 150 events with top 1% e_2 -eccentricity,
3. and an averaged event (smoothed profile).

Those initial conditions are consecutively run through the v-USPhydro and BBMG code. The results for the nuclear modification factor and the high- p_T elliptic flow are shown in Figs. 3 and 4. Please note that the reference point chosen for all scenarios is $R_{AA}(p_T = 10 \text{ GeV}) = 0.185$. In Fig. 4 we compare three different methods to determine the high- p_T elliptic flow: the arithmetic mean $\langle v_n \rangle$, the root

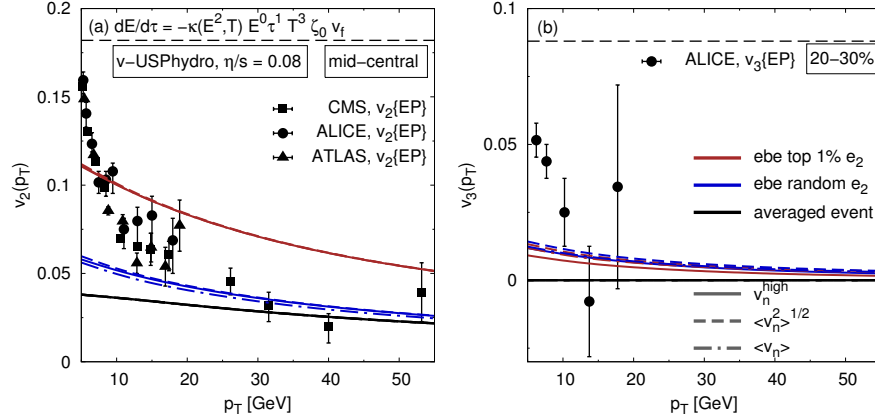


Fig. 4 The high- p_T v_2 (left) and v_3 (right) calculated via the arithmetic mean, the root mean square, and Eq. (7) for the three e_2 -eccentricity selections of the centrality classes 20-30% and compared to the measured data at $\sqrt{2.75}$ TeV LHC energy [68, 69, 70].

mean square $\langle v_n^2 \rangle^{1/2}$, and v_n^{high} given by

$$v_n^{\text{high}} = \frac{\langle v_n^{\text{low}} v_n^{\text{high}}(p_T) \cos[n(\psi_n^{\text{low}} - \psi_n^{\text{high}}(p_T))] \rangle_{\text{events}}}{\sqrt{\langle v_n^{2,\text{low}} \rangle_{\text{events}}}} \quad (7)$$

which is used by experiment [66, 67].

Fig. 3 shows that there is almost no difference between the event-by-event and smoothed initial conditions for the nuclear modification factor. Thus, R_{AA} is independent of the e_2 -eccentricity distribution of the background medium.

Fig. 4 demonstrates that the high- p_T v_2 is proportional to the low- p_T v_2 (which is the largest for the top 1% e_2 events) and that the width of the low- p_T v_2 -distribution influences the high- p_T v_2 . Besides that, the event-by-event fluctuations enhance the high- p_T v_2 , depending on the e_2 -eccentricity selection. The yields for the arithmetic mean $\langle v_n \rangle$, the root mean square $\langle v_n^2 \rangle^{1/2}$, and the v_n^{high} are similar. Fig. 4 exhibits that e_2 and e_3 are anticorrelated as for the low- p_T bulk medium [71, 72].

7 Conclusions

By reviewing the challenges, results, and open problems of jet physics in heavy-ion collisions, discussing the main ideas and concepts as well as most recent results of the nuclear modification factor and the high- p_T elliptic flow, I showed that jets are important tools to probe heavy-ion collisions. Unfortunately, it has not yet been possible to disentangle the underlying theory (pQCD or AdS/CFT) with these measurements but we must find a way. Jet physics in heavy-ion collision clearly shows

that the results obtained are influenced both by the background medium and the jet-energy loss description.

8 Acknowledgements

The author thanks C. Greiner, M. Gyulassy, J. Noronha-Hostler, J. Noronha, F. Senzel, and J. Xu for the fruitful collaboration as well as U. Heinz and C. Shen for providing their hydrodynamic field grids. This work was supported through the Bundesministerium für Bildung und Forschung under project number 05P2015, the Helmholtz International Centre for FAIR within the framework of the LOEWE program (Landesoffensive zur Entwicklung Wissenschaftlich-Ökonomischer Exzellenz) launched by the State of Hesse. The author thanks the organizers of the Symposium on "New Horizons in Fundamental Physics" for an inspiring workshop celebrating Walter Greiner's 80th birthday.

References

1. J. D. Bjorken, Phys. Rev. D **27**, 140 (1983).
2. M. Gyulassy and M. Plumer, Phys. Lett. B **243**, 432 (1990).
3. X. N. Wang and M. Gyulassy, Phys. Rev. Lett. **68**, 1480 (1992).
4. B. G. Zakharov, JETP Lett. **63**, 952 (1996).
5. R. Baier, Y. L. Dokshitzer, A. H. Mueller, S. Peigne and D. Schiff, Nucl. Phys. B **483**, 291 (1997).
6. I. Arsene *et al.* [BRAHMS Collaboration], Nucl. Phys. A **757**, 1 (2005).
7. K. Adcox *et al.* [PHENIX Collaboration], Nucl. Phys. A **757**, 184 (2005).
8. B. B. Back *et al.*, Nucl. Phys. A **757**, 28 (2005).
9. J. Adams *et al.* [STAR Collaboration], Nucl. Phys. A **757**, 102 (2005).
10. J. Adams *et al.* [STAR Collaboration], Phys. Rev. Lett. **91**, 072304 (2003).
11. A. Adare *et al.* [PHENIX Collaboration], Phys. Rev. C **78**, 014901 (2008).
12. H. G. Baumgardt, J. U. Schott, Y. Sakamoto, E. Schopper, H. Stoecker, J. Hofmann, W. Scheid and W. Greiner, Z. Phys. A **273**, 359 (1975).
13. J. Hofmann, H. Stoecker, U. W. Heinz, W. Scheid and W. Greiner, Phys. Rev. Lett. **36**, 88 (1976).
14. B. Betz, J. Noronha, G. Torrieri, M. Gyulassy and D. H. Rischke, Phys. Rev. Lett. **105**, 222301 (2010).
15. M. Gyulassy, P. Levai and I. Vitev, Phys. Rev. Lett. **85**, 5535 (2000).
16. M. Djordjevic and M. Gyulassy, Nucl. Phys. A **733**, 265 (2004).
17. S. Wicks, W. Horowitz, M. Djordjevic and M. Gyulassy, Nucl. Phys. A **783**, 493 (2007).
18. R. Baier, Y. L. Dokshitzer, A. H. Mueller, S. Peigne and D. Schiff, Nucl. Phys. B **484**, 265 (1997).
19. U. A. Wiedemann, Nucl. Phys. B **588**, 303 (2000).
20. J. w. Qiu and G. F. Sterman, Nucl. Phys. B **353**, 105 (1991).
21. P. B. Arnold, G. D. Moore and L. G. Yaffe, JHEP **0111**, 057 (2001).
22. J. Adams *et al.* [STAR Collaboration], Phys. Rev. Lett. **91**, 172302 (2003).
23. S. S. Adler *et al.* [PHENIX Collaboration], Phys. Rev. C **75**, 024909 (2007).
24. I. Vitev and M. Gyulassy, Phys. Rev. Lett. **89**, 252301 (2002).

25. M. Gyulassy and L. McLerran, Nucl. Phys. A **750**, 30 (2005).
26. E. Shuryak, Prog. Part. Nucl. Phys. **53**, 273 (2004).
27. P. Romatschke and U. Romatschke, Phys. Rev. Lett. **99**, 172301 (2007).
28. M. Gyulassy, Talk given at the HCBM 2010 Conference, Budapest, Hungary, August 2010.
29. J. M. Maldacena, Adv. Theor. Math. Phys. **2**, 231 (1998) [Int. J. Theor. Phys. **38**, 1113 (1999)].
30. S. S. Gubser, D. R. Gulotta, S. S. Pufu and F. D. Rocha, JHEP **0810**, 052 (2008).
31. P. M. Chesler, K. Jensen, A. Karch and L. G. Yaffe, Phys. Rev. D **79**, 125015 (2009).
32. P. M. Chesler, K. Jensen and A. Karch, Phys. Rev. D **79**, 025021 (2009).
33. M. Gyulassy, A. Buzzatti, A. Ficnar, J. Noronha and G. Torrieri, EPJ Web Conf. **13**, 01001 (2011).
34. A. Adare *et al.* [PHENIX Collaboration], Phys. Rev. Lett. **105**, 142301 (2010).
35. W. A. Horowitz and M. Gyulassy, Nucl. Phys. A **872**, 265 (2011).
36. B. Betz, M. Gyulassy and G. Torrieri, Phys. Rev. C **84**, 024913 (2011).
37. S. Pal and M. Bleicher, Phys. Lett. B **709**, 82 (2012).
38. W. A. Horowitz, J. Phys. G **35**, 044025 (2008).
39. B. Betz and M. Gyulassy, Phys. Rev. C **86**, 024903 (2012).
40. B. Betz and M. Gyulassy, JHEP **1408**, 090 (2014) [JHEP **1410**, 043 (2014)].
41. H. Liu, K. Rajagopal and U. A. Wiedemann, JHEP **0703**, 066 (2007).
42. R. Baier, A. H. Mueller and D. Schiff, Phys. Lett. B **649**, 147 (2007).
43. T. Renk and J. Ruppert, Phys. Rev. C **72**, 044901 (2005).
44. N. Armesto, C. A. Salgado and U. A. Wiedemann, Phys. Rev. C **72**, 064910 (2005).
45. J. Xu, J. Liao and M. Gyulassy, Chin. Phys. Lett. **32**, no. 9, 092501 (2015).
46. A. Buzzatti and M. Gyulassy, Nucl. Phys. A **904-905**, 779c (2013).
47. A. Buzzatti and M. Gyulassy, Nucl. Phys. A **910-911**, 490 (2013).
48. C. Shen, U. Heinz, P. Huovinen and H. Song, Phys. Rev. C **84**, 044903 (2011); Phys. Rev. C **82**, 054904 (2010).
49. M. Luzum and P. Romatschke, Phys. Rev. C **78**, 034915 (2008) [Erratum-ibid. C **79**, 039903 (2009)].
50. Z. Xu and C. Greiner, Phys. Rev. C **71**, 064901 (2005).
51. A. Adare *et al.* (PHENIX Collaboration), Phys. Rev. Lett. **101**, 232301 (2008).
52. J. Jia (ATLAS Collaboration), J. Phys. G **38**, 124012 (2011).
53. S. Chatrchyan *et al.* (CMS Collaboration), Eur. Phys. J. C **72**, 1945 (2012).
54. A. Ficnar, J. Noronha and M. Gyulassy, J. Phys. G **38**, 124176 (2011).
55. S. I. Finazzo, R. Rougemont, H. Marrochio and J. Noronha, JHEP **1502**, 051 (2015).
56. J. Xu, A. Buzzatti and M. Gyulassy, JHEP **1408**, 063 (2014).
57. D. Molnar and D. Sun, Nucl. Phys. A **910-911**, 486 (2013).
58. B. Betz, F. Senzel, C. Greiner and M. Gyulassy, arXiv:1512.07443 [hep-ph].
59. B. Betz, J. Noronha-Hostler, J. Noronha, M. Gyulassy, in preparation.
60. B. Abelev *et al.* [ALICE Collaboration], Phys. Lett. B **720**, 52 (2013).
61. S. Chatrchyan *et al.* [CMS Collaboration], Eur. Phys. J. C **72**, 1945 (2012).
62. G. Aad *et al.* [ATLAS Collaboration], JHEP **1311**, 183 (2013).
63. J. Noronha-Hostler, B. Betz, J. Noronha and M. Gyulassy, arXiv:1602.03788 [nucl-th].
64. J. Noronha-Hostler, G. S. Denicol, J. Noronha, R. P. G. Andrade and F. Grassi, Phys. Rev. C **88**, 044916 (2013).
65. J. Noronha-Hostler, J. Noronha and F. Grassi, Phys. Rev. C **90**, no. 3, 034907 (2014).
66. G. Aad *et al.* [ATLAS Collaboration], Phys. Rev. C **92**, no. 3, 034903 (2015).
67. K. Aamodt *et al.* [ALICE Collaboration], Phys. Lett. B **708**, 249 (2012).
68. B. Abelev *et al.* [ALICE Collaboration], Phys. Lett. B **719**, 18 (2013).
69. S. Chatrchyan *et al.* [CMS Collaboration], Phys. Rev. Lett. **109**, 022301 (2012).
70. G. Aad *et al.* [ATLAS Collaboration], Phys. Lett. B **707**, 330 (2012).
71. H. Niemi, G. S. Denicol, H. Holopainen and P. Huovinen, Phys. Rev. C **87**, no. 5, 054901 (2013).
72. E. Retinskaya, M. Luzum and J. Y. Ollitrault, Phys. Rev. C **89**, no. 1, 014902 (2014).